Study of Potassium *O*,*O*′-Dibutyldithiophosphate Combining DFT, ^{31}P CP/MAS NMR and Infrared Spectroscopy

Pär Hellström,[†] Anna-Carin Larsson,*[,‡] Andreas Fredriksson,[‡] Allan Holmgren,[‡] and Sven Öberg[†]

Department of Mathematics, Luleå University of Technology, SE 971 87 LULEÅ, SWEDEN, and Division of Chemistry, Department of Chemical Engineeering and Geosciences, Luleå University of Technology, SE 971 87 LULEÅ, SWEDEN

Received: June 9, 2008; Revised Manuscript Received: September 9, 2008

Dithiophosphates are used in many different industrial applications. To explain their functions and properties in these applications, a fundamental understanding on a molecular level is needed. Potassium *O*,*O*′-Dibutyldithiophosphate and its anion have been investigated by means of a combination of DFT and ^{31}P CP/MAS NMR and infrared spectroscopy. Several low-energy conformations were studied by DFT. Three different conformations with significantly different torsion angles of the O−C bond relative to the O−P−O plane were selected for further studies of infrared frequencies and ^{31}P NMR chemical-shift tensors. A good agreement between theoretical and experimental results was obtained, especially when the IR spectra or ^{31}P chemical shift tensor parameters of all three conformations were added, indicating that, because of the low energy difference between the conformations, the molecules are rapidly fluctuating between them.

1. Introduction

Dialkyldithiophosphates (DTP), $[(RO)_2PS_2]^-$, are used in many different industrial applications, for example as insecticides and pesticides[1] or for fabrication of nanoclusters.[2,3] One important usage for the ionic salts of DTP is as a collector in the froth flotation of sulfide minerals[4] but they have also been proposed as chelating agents for heavy metal ions to clean water from contaminants.[5] Various metal DTP complexes are used as antiwear and antioxidant additives in motor oils.[3,6,7] The versatility of applications of DTPs, as well as their ability to combine with metal ions into a variety of coordination complexes, have led to a large interest in their structure and the factors governing the properties of DTP complexes. The crystal structure of a wide range of metal DTPs has been determined by single-crystal X-ray diffraction and also studied with various other spectroscopic techniques.[8−10] Larsson et al. have published a work about correlations between ^{31}P chemical shift tensors and structural parameters in a number of metal DTP complexes as well as on a dimethyldithiophosphate fragment, combining ab initio calculations with experimental ^{31}P CP/MAS NMR,[11] and Billes et al. recently published a work on potassium diethyldithiophosphate combining computer simulations of vibrational modes with experimental IR studies.[12] In recent years, the interest for theoretical studies of DTP has increased, especially in the field of tribology, and has led to numerous articles trying to describe the molecular properties and behavior of zinc DTP.[6,13,14] To explain the functions and properties of DTP in its different applications, a fundamental understanding of DTP on a molecular level is needed. In this work, the dibutyldithiophosphate anion (DBDTP) and its potassium salt (KDBDTP) are studied using both computational methods (DFT) as well as experimental techniques such as infrared spectroscopy and solid-state ^{31}P CP/MAS NMR. The results from DFT calculations of optimized geometries, vibrational frequencies, and ^{31}P chemical shift tensors are presented and compared with experimental results. The approach of combining theoretical and experimental methods gives new insight into the interpretation of experimental data and develops the computational methods to better account for the experimental data.

2. Materials and Methods

2.1. Materials. The potassium dithiophosphate salt used was of high purity, and delivered by Cheminova A/S, under the name Danafloat 145.

2.2. Infrared Measurements. Diffuse reflectance infrared Fourier transform (DRIFT) and transmission infrared analyses were performed using a Bruker IFS 66 v/S FTIR spectrometer under low pressure (1 mBar). The instrument was equipped with a DTGS (deuterated triglycine sulfate) detector allowing analysis down to 400 cm^{-1}.

In the DRIFT measurements, the solid sample was diluted in a nonabsorbing matrix (KBr powder) to avoid any spectral artifacts that otherwise can occur in regions of high absorptivity. The weight ratio between sample and KBr was between 1 and 5 mg of sample to ∼300 mg of KBr.

Infrared transmission spectra were recorded using a vacuum cell (6 μm spacers, Viton gaskets and CaF_2 windows) for the sample. The concentration of DBDTP was <0.05 M. CaF_2, is a good infrared transmitting material for aqueous solutions but has a wavenumber cut off at 950 cm^{-1}. The infrared absorption of water was strong in the OH-stretching region but could be subtracted from the sample spectrum using a spectrum of the pure solvent to clearly reveal the C−H stretching region of the DBDTP spectrum.

2.3. NMR Measurements. Solid-state ^{31}P CP/MAS NMR measurements were performed on a Chemagnetics/Varian Infinity CMX-360 spectrometer (B_0 = 8.46 T). The isotropic

* To whom correspondence should be addressed. E-mail: anna-carin.v.larsson@ltu.se. Fax: +46(0)920491199. Phone: +46(0) 920491694 (A. L.), Par.Hellstrom@sonyericsson.com (P. H.), andreas.fredriksson@lkab.com (A. F.), allan.r.holmgren@ltu.se (A. H.), sven.oberg@ltu.se (S. O.).

[†] Department of Mathematics.

[‡] Division of Chemistry.

10.1021/jp805058a CCC: $40.75
Published on Web 10/23/2008

chemical shift (on the deshielding δ-scale) was given with respect to 85% H_3PO_4 (0 ppm), which was mounted in a short capillary glass tube (∅ 1 mm) and placed in a 7.5 mm rotor to minimize errors due to differences in magnetic susceptibility. Simulations of the ^{31}P chemical shift anisotropy (CSA) parameters were performed with a *Mathematica*-based program developed by Levitt and co-workers.[15] The input file to the program consists of the experimental sideband intensities, the experimental spinning frequency, the Larmor frequency, and the experimental noise variance. The program plots the χ^2 statistics as a function of the two CSA parameters δ_{aniso} and η, with a minimum at certain values of these two parameters. Sideband intensities were measured with the deconvolution method using the inbuilt *Spinsight* spectrometer software. Values of δ_{aniso} and η were obtained from simulations at two different spinning frequencies. Their mean value and mean statistical errors were calculated.[11] The principal values of the chemical shift tensor were recalculated from δ_{aniso} and η according to the following equations:

$$\delta_{iso} = (\delta_{xx} + \delta_{yy} + \delta_{zz})/3 \quad (1)$$

$$\delta_{aniso} = \delta_{zz} - \delta_{iso} \quad (2)$$

$$\eta = (\delta_{yy} - \delta_{xx})/\delta_{aniso} \quad (3)$$

with δ_{xx}, δ_{yy}, and δ_{zz} defined according to $|\delta_{zz} - \delta_{iso}| \geq |\delta_{xx} - \delta_{iso}| \geq |\delta_{yy} - \delta_{iso}|$.[15]

The parameters Ω (span) and κ (skew) are also used to describe the tensors, with the following definitions:[16]

$$\Omega = \delta_{11} - \delta_{33} = \sigma_{33} - \sigma_{11} \quad (4)$$

$$\kappa = 3(\delta_{22} - \delta_{iso})/\Omega = 3(\sigma_{iso} - \sigma_{22})/\Omega \quad (5)$$

with $\delta_{11} \geq \delta_{22} \geq \delta_{33}$ on the deshielding δ-scale, and $\sigma_{33} \geq \sigma_{22} \geq \sigma_{11}$ on the shielding σ scale. The confidence intervals of the chemical shift tensor parameters were calculated with the partial derivative method, using the confidence intervals of δ_{aniso} and η.

2.4. Calculations

Density functional theory (DFT) implemented in the *NW Chem 5.0* program was used for geometrical optimization and calculation of the vibrational frequencies and intensities for the DBDTP anion and the KDBDTP salt as well as the absolute shielding of the ^{31}P nuclei for KDBDTP.

The alkyl chains of both DBDTP and KDBDTP have a number of different conformations. Jiang et al. calculated the optimized geometrical structures and vibrational frequencies of the dimethyl-DTP anion and suggested three stable conformations of the OMe chains.[6] These three structures all have the PS_2 plane orthogonal to the PO_2 plane. The difference between the three structures is due to the rotation around the P−O bond making the three molecules belong to either the C_{2v}, C_2, or C_1 symmetry group. In this study, we use the same three basic structures as starting points. After a geometrical optimization, the OMe chains were substituted for ethyl chains by replacing a hydrogen atom on each chain with a CH_3 group. Now the structures were geometrically optimized again. The procedure of adding CH_3 groups at the end of the hydrocarbon chains was repeated three times until butyl chains were achieved. At each step, if possible, the highest possible symmetry was maintained. From the original potassium methyldithiophosphate with C_{2v} symmetry four KDBDTP molecules with C_2 symmetry were analyzed plus one preserving the C_{2v} symmetry. Starting with the potassium methyl dithiophosphate with C_2 symmetry, 15 KDBDTP molecules with maintained symmetry were constructed. In both of these 2 cases, redundant structures were not considered. Such a reduction of numbers could not be performed when potassium methyldithiophosphate with C_1 symmetry was used as a starting point.

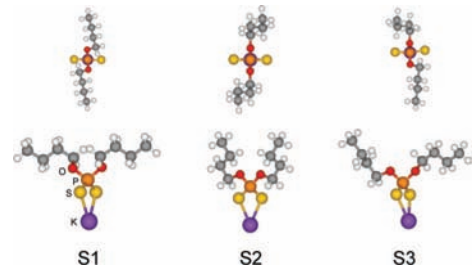

Figure 1. Two views of the lowest energy conformations of KDBDTP from the three categories, where S3 has the lowest energy.

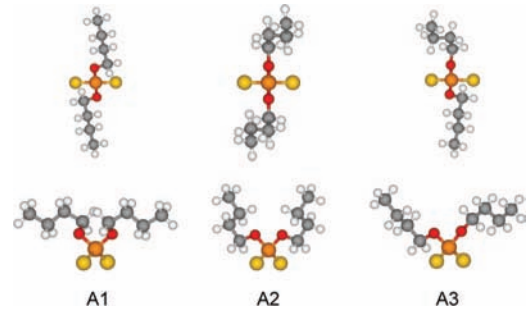

Figure 2. Two views of the lowest energy conformations of DBDTP from the three categories, where A2 has the lowest energy.

A total of 135 KDBDTP molecules of C_1 symmetry were constructed and geometrically optimized, all of them just differing in the geometry of their hydrocarbon chains. In all of these preliminary calculations, the applied basis set was DZVP together with the B3LYP functional.[17] From each of the originating three symmetry groups, the three most energetically preferable structures were selected. Hence, three groups with different rotation of the P−O bond, each with three structures, were obtained. These final geometrical structures were then checked for convergence by means of the larger 6−311++G(2d, 2p) basis set.[18]

The initial structures of the DBDTP anion (charge −1) were obtained from these nine optimized conformations by removal of the potassium atom and then performing a geometrical optimization using the 6−311++G(2d, 2p) basis set. Accordingly, these calculations resulted in six structures having the lowest energy of their category. These structures are referred to as A1, A2, and A3 for the anion and S1, S2, and S3 for the salt. S1 is the salt corresponding to the A1 anion S2 to A2 and so forth as seen in Figures 1 and 2. These three conformations were chosen because they are the three with the lowest total energy and they represent three distinctly different torsion angles between the two O−C bonds and the O−P−O plane.

To visualize the calculated discrete vibrational frequencies and their corresponding infrared intensities, the following formula

$$f(x) = \sum_{k=1}^{n} \alpha_i e^{-\beta(x - \gamma_i)^2} \quad (6)$$

was used. In this formula, α_i (peak height) is the infrared intensity associated with the ith vibrational frequency, β is a scale factor to determine the width of each Gaussian function,

TABLE 1: Geometrical Details of the Three Conformations of the KDBDTP Salt (S) and Calculated Changes with Respect to the Anion (A)[a]

angle/length	S1	S2	S3	A1 → S1	A2 → S2	A3 → S3
P−O (Å)	2.02	2.03	2.03	−0.036	−0.034	−0.031/−0.038
P−S (Å)	1.64	1.63	1.64	0.023	0.023	0.022/0.023
S−P−S (°)	119.4	116.7	118.0	−3.19	−3.06	−3.16
O−P−O (°)	103.0	94.1	98.6	3.48	2.29	3.00

[a] 6-311G++(2d, 2p) was used as basis set together with the B3LYP functional.

here set to 1000 to get narrow lines, and γ_i is the *i*th vibrational frequency.

The calculations of the ^{31}P shielding tensors are given in the shielding scale (σ), whereas the experimentally determined chemical shift tensors (CST) are given relative to the shielding of a reference nucleus (85% H_3PO_4), and reported on the deshielding scale (δ). To simplify the comparison between experimental and calculated data, the DFT tensor parameters have been converted to the deshielding scale but not adjusted to the same relative scale as the experimental data.

The ^{31}P shielding tensors were also checked for convergence using Gaussian and the larger basis sets (2df, 2pd) and (3df, 3pd).

3. Results and Discussion

3.1. Geometry Optimization. In Figure 1, the three low energy conformations of the KDBDTP salt are shown. The torsion angles of the two O−C bonds with respect to the O−P−O plane are 65.3° and 179.6° for the S1 and S2 conformations respectively, whereas the torsion angles of S3 are 64.2° and 178.2°, respectively. The two K−S distances are 2.99 and 2.98 Å for the S1, S2, and S3 conformations, respectively. The S3 conformation was found to have lowest total energy in contrast to the DBDTP anion where the A2 conformation is the optimal. S1 and S2 have respectively 2.05 and 2.51 kJ mol^{-1} higher energy than S3. The same energy order was obtained by Jiang et al., in their study of the Zn(SH)[$(MeO)_2PS_2$ system.[6]

There exist several low-energy conformations due to the small energy differences between the various conformations of the hydrocarbon chains. Here, only the three conformations with different torsion angles of the O−C bonds with respect to the O−P−O plane are presented. The reason is simply that these conformations led to the largest differences in the geometry of the PS_2O_2-tetrahedron, and hence, the largest effect on the spectroscopic results.

The three geometrically optimized conformations of the DBDTP anion are shown in Figure 2. The torsion angles of the two O−C bonds with respect to the O−P−O plane are for the A1 conformation both 67.5°, and for the A2 conformation both 179.4°. The A3 conformation has, of course, two different torsion angles, 68.7 and 178.5°, respectively. Jiang et al. reported that the conformation of the dimethyl-DTP anion with a torsion angle of 180° about the P−O bond was the energetically optimal one.[6] This conformation is analogous to our A2, which is found to be the most stable structure of DBDTP reported here (Figure 2). The A3 and A1 conformations have respectively 0.63 and 3.97 kJ mol^{-1} higher energy than A2.

The P−O bond lengths in S1 and S2 are shorter by 0.036 and 0.034 Å respectively, compared with the corresponding bond lengths in the A1 and A2 conformations. A transition from A3 to S3 implies that the two P−O bonds became shorter by 0.031 and 0.038 Å respectively, where the latter value refers to the side where the O−C bond lies within the O−P−O plane. The P−S bond lengths increased by 0.023 Å for the A1 → S1 and A2 → S2 transitions and by 0.022 and 0.023 Å for A3 → S3. All other bond lengths change with less than 0.02 Å. Billes and Holmgren[12] showed that the addition of a potassium ion to the EtDTP anion increases the P−S bonds and decreases the bond lengths of the P−O bonds, in accordance with the results presented here. A similar result was obtained in the study of Jiang et al.[6] when Zn(SH) was added to the methyl DTP anion.

The O−P−O angle was increased by 3.48, 2.29, and 3.00° when potassium was added to A1, A2, and A3 respectively, whereas the S−P−S angle, being directly affected by the potassium ion, showed a decrease by 3.19, 3.06, and 3.16° for the A1 → S1, A2 → S2, and A3 → S3 transitions, respectively. The corresponding angle was decreased by 3.6° for EtDTP,[12] compared to 3.19° obtained here, upon addition of the potassium ion. Similarly, adding Zn(SH) to the MeDTP anion resulted in a decrease of the S−P−S angle by 10°.[6] Besides the previously mentioned angles, the only one that was significantly affected by the presence of the potassium atom was the P−O−C angle, which increased by 2.3° for the A2 → S2 transition. In A3 → S3, it is only the P−O−C angle perpendicular to the PS_2 plane that is affected (increased by 2.07°). All other changes in bond angles were less than 0.8°. A summary of the changes in bond lengths and angles discussed is shown in Table 1 together with geometrical data for the S1, S2, and S3 conformations.

3.2. Vibrational Modes. Figure 3 shows the calculated infrared spectra of the CH_3/CH_2 stretching region between 3100 and 2800 cm^{-1} of the DBDTP anion (A) and the KDBDTP salt (S). Spectra of the three S and A conformations of the hydrocarbon chains are shown in pairs to facilitate the comparison. The hydrocarbon chains are only marginally influenced by the presence of the metal atom; the anion shows lower calculated vibrational frequencies than the corresponding KDBDTP by about 0.5%. The relative intensities of the vibrations change when the potassium atom is added, and some intensities decrease to almost zero.

Figure 4 shows the experimental IR spectra of the DBDTP anion (transmission IR) and KDBDTP salt (DRIFT). There exist no absolute relations between the intensities of the vibrational frequencies in the calculated spectra and the experimental spectra. The differences between the calculated and the measured vibrational frequencies are less than 5%, which is normal for these kinds of calculations.[19] Hellström et al.[19] showed that vibrational frequencies often are overestimated by 5% when calculated with DFT using the DZVP basis set together with the B3LYP functional. This overestimation is a consequence of the method and often corrected applying a scale factor. This correction is not applied here, but all vibrational frequencies reported are unscaled.

Although the vibrational frequencies are unscaled, they are in good agreement with experimental results. Notice that in this region a 30 cm^{-1} shift represents a difference of about 1%. The experimental DRIFT spectrum has five vibrational bands, to be compared with all the frequency lines in the calculated spectra

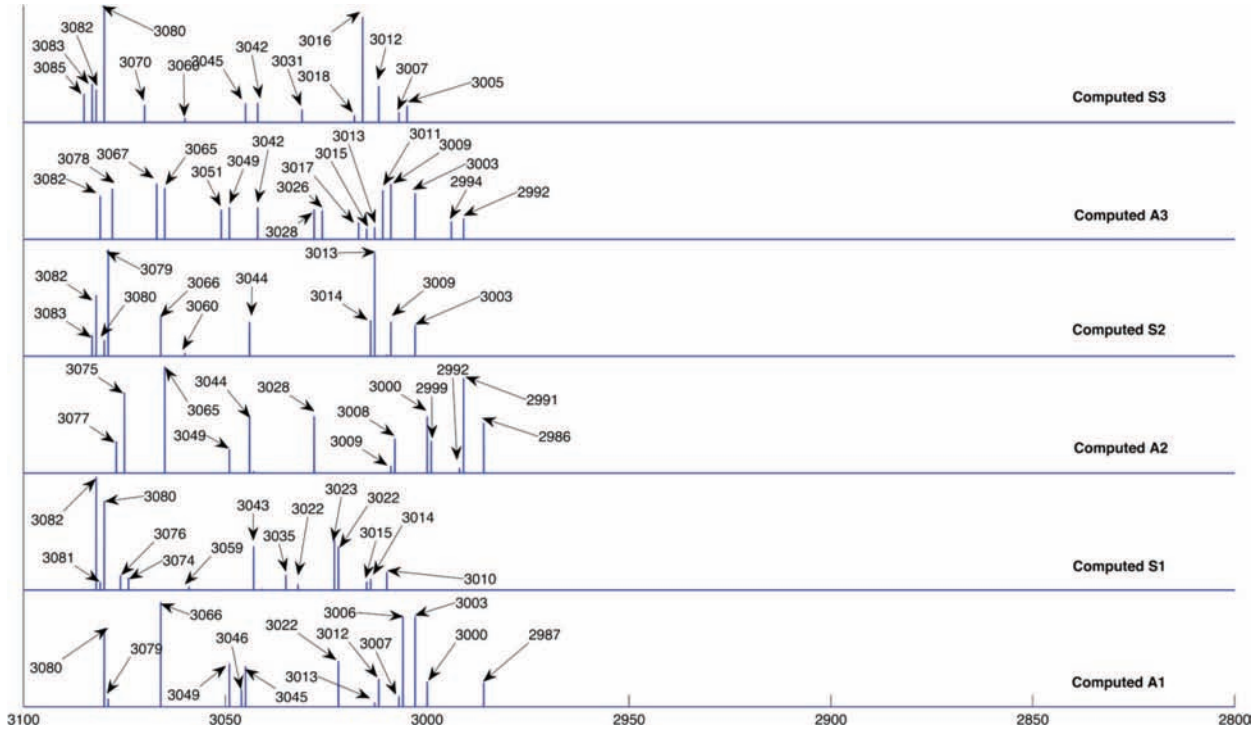

Figure 3. Calculated line spectra of the A1−A3 and S1−S3 geometrical conformations, in the 3100−2800 cm^{-1} region. 6−311++G(2d, 2p) was used as basis set together with the B3LYP functional.

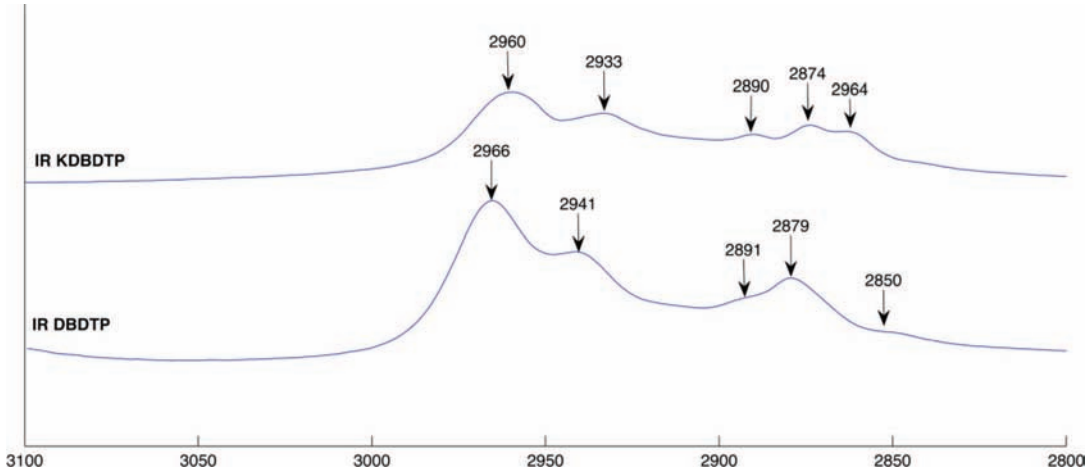

Figure 4. Experimental IR spectra of DBDTP and KDBDTP in the spectral region 3150−2800 cm^{-1}.

of S1−S3. The number of bands in the experimental IR spectrum, and their line widths are best represented by the sum of the calculated frequencies in S1−S3, indicating that all three conformations contribute to the experimental spectrum as seen in Figure 4. This is a reasonable assumption, considering the small energy differences between the conformations.

Some of the vibrations in the 1200−500 cm^{-1} region should be more influenced by the presence of a metal ion, especially vibrations involving the P−S, P−O, and C−O bonds. Classifications of the vibrational modes are shown in Table 2. Figures 5 and 6 show experimental IR spectra as well as computed S and A spectra. The three low energy conformations are so close in energy that the best representation of the real spectrum is probably an average of the individual spectra. Even so, we choose to report them separately for a more detailed discussion.

The assignments in Table 2 are made using the following acronyms stretching (str), rocking (rock), wagging (wag), and twisting (tw). Because the two hydrocarbon chains are twisted differently around the P−O axis in the A3 and S3 conformations, the vibrational frequencies often appear in pairs that are close in vibrational frequency but have different vibrational modes assigned to them. Often just one of the hydrocarbon chains (α and β in Table 2) contributes to the vibrational intensity, whereas the other one is of minor importance. In Table 2, α and β refer to the left and right hydrocarbon chains respectively of A3 and S3, as seen in Figures 1 and 2. In many of the vibrational modes, both hydrocarbon chains are either vibrating in phase, that is, all CH_2 entities having the same position in the two chains vibrate symmetrically with respect to each other, or out of phase, where the CH_2 entities in the two chains vibrate asymmetrically with respect to each other. This is marked in Table 2 as CH chains in/out of phase.

The difference in frequency between the conformations of the anion and the potassium salt is less than 12 cm^{-1} in the 1200−950 cm^{-1} region. As for the C−H stretching region, there is a good agreement between the sum of calculated vibrational frequencies (A1−A3 and S1−S3, respectively) and the number

TABLE 2: Calculated Frequencies of DBDTP and KDBDTP and Their Corresponding Assignments[b]

A1	A2	A3	S1	S2	S3	assignments[a]
575	537	550	575	532	547	P−S, P−O sym str, CH_2 rock
	542			542		P−S, P−O asym str CH_2 rock
670	647	666	650	620	641	P−S, P−O asym str
711			726			CH_2, CH_3 rock, P−O, P−S sym str
723	717		737	734		CH_2, CH_3 rock, P−O asym str
768	738		782	743		CH_2, CH_3 rock. P−O, P−S sym str
770	770		795	788		CH_2, CH_3 rock, P−O asym str
	786			807		CH_2, CH_3 rock, P−O, P−S sym str
		714			736	α CH_2, CH_3 rock, P−O asym str
		727			739	*β* CH_2, CH_3 rock, P−O asym str
		769			789	α CH_2, CH_3 rock, tw, P−O, C−O asym str
		778			795	*β* CH_2, CH_3 rock, P−O asym str
836	838		838	840		CH_2, CH_3 rock, C−C str, CH-chains out of phase
836	838		838	840		CH_2, CH_3 rock, C−C str, CH-chains in phase
		839			838	*β* CH_2 rock, C−C str
		841			839	α CH_2, CH_3 rock, C−C str
		879			895	α CH_2, CH_3 tw, rock, P−O asym str
		888			900	*β* CH_2, CH_3 tw, rock, P−O asym str
877	881		894	899		CH_2, CH_3 tw, rock, P−O asym str
880	886		894	902		CH_2, CH_3 tw, rock P−O sym str
970	968	971	968	973	973	CH_2, CH_3 tw, rock P−O, C−O asym str, C−C str
970		975	972		978	CH_2, CH_3 tw, rock P−O, C−O sym str, C−C str
	977			982		CH_2, CH_3 wag, C−C str, CH-chains in phase
978	983		979	986		CH_2, CH_3 tw, rock
979	988		980	995		CH_2, CH_3 tw, rock
		980			982	CH_2, CH_3 tw, rock, *β* dominant
		986			988	CH_2, CH_3 tw, rock, α dominant
1028	1029	1029	1025	1027	1024	C−C str, P−O, C−O asym str, CH_3 wag
1029	1036	1034	1027	1039	1032	C−C str, P−O, C−O sym str, CH_3 wag
1067	1076	1070	1062	1067	1063	C−C, C−O asym str, CH_2 wag
1073	1097	1085	1066	1088	1073	C−C asym, C−O sym str, CH_2 wag
1138			1139			C−C asym, C−O sym str, CH_2 wag
1138			1140			C−C, C−O asym str, CH_2 wag
	1138			1139		C−C str, CH_2, CH_3 rock
	1142			1141		C−C str, CH_2, CH_3 rock
		1139			1138	*β* C−C str, CH_2, CH_3 wag
		1141			1140	α C−C str, CH_2, CH_3 wag
1174	1174		1172	1175		CH_2 rock, CH-chains in phase
1174	1174		1173	1175		CH_2 rock, CH-chains out of phase
		1174			1173	*β* CH_2, CH_3 rock
		1174			1174	α CH_2, CH_3 rock

[a] Some of the assignments are seemingly identical, but different CH_2 entities in the alkyl chains may vibrate with different frequencies.[19] [b] 6-311++G(2d, 2p) was used as basis set together with the B3LYP functional.

of absorption bands and their line widths detected by IR spectroscopy, indicating that all three conformations contribute to the experimental spectra, as seen in Figures 5 and 6.

The effects of the metal atom in the 900−500 cm^{-1} region are larger. For example, the asymmetric P−O and P−S stretching modes around 650 cm^{-1} are shifted downward by 20−25 cm^{-1} when the potassium ion is introduced. The agreement between experimental DRIFT and calculated line spectra of S1−S3 is also good in this spectral region, provided that the calculated spectra of all three conformations are added together. However, the strong vibrational frequencies in the region 650−620 cm^{-1} are missing in the experimental spectrum, and the calculated spectrum has no vibrational frequencies in the region around 709 cm^{-1}, where a strong band is seen in the experimental spectrum. However, it can not be excluded that the calculated vibrations at 650, 620, and 641 cm^{-1} corresponds to the experimentally obtained band at 709 cm^{-1} because the scaling function is unknown. Scaling is reasonable because of the difference in experimental and theoretical environment of the formula unit.

The agreement between experimental and calculated vibrational frequencies for A1−A3 is impossible to assess due to the frequency cutoff of the CaF_2 window at 950 cm^{-1}.

4.3. ^{31}P Chemical Shift Anisotropy Analysis. The conformations S1−S3 represent the potassium salt of the DTP in the solid state, and the ^{31}P chemical shift tensor parameters of these conformations can be compared with the experimental NMR results for the KDBDTP. The experimental ^{31}P CP/MAS NMR data of the KDBDTP salt are presented in Table 3 together with the results from the DFT calculations. To simplify the comparison between experimental and calculated data, the calculated DFT tensor parameters have been converted from the shielding scale (σ) to the deshielding scale (δ) but not adjusted to the same relative scale as the experimental data. The experimental and calculated properties are in quite good agreement for all three conformations (S1−S3). The lowest energy conformation S3 seems to give a slightly better fit to the experimental values than either S1 or S2. However, the energy differences between the S1−S3 conformations are small, and as the IR calculations indicate, all three conformations contribute to the IR spectrum, and, therefore, it is reasonable to assume that all three conformations should be present also in the NMR experiment. The experimental ^{31}P CP/MAS NMR spectrum, however, show only one peak. One possible explanation is that all three conformations happen to have the same experimental chemi-

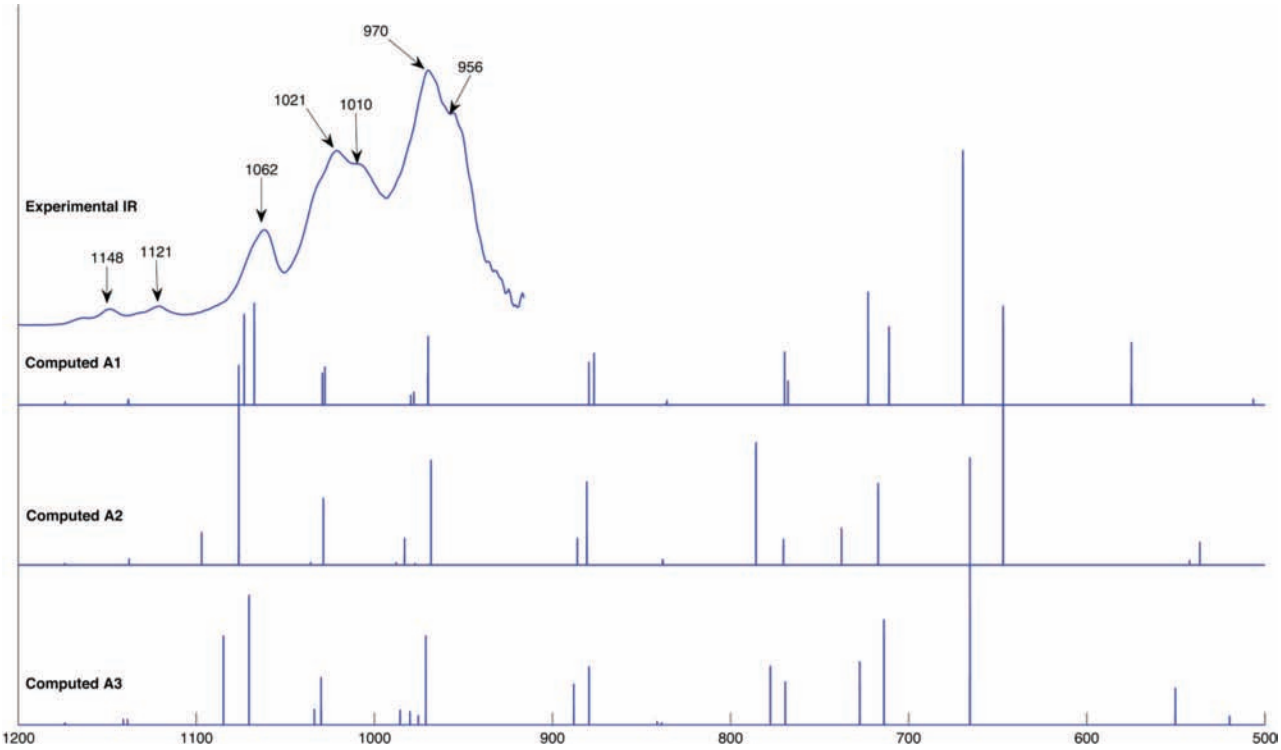

Figure 5. Calculated and experimental vibrational spectra of the A1−A3 conformations in the 1200−500 cm^{-1} region. 6−311++G(2d, 2p) was used as basis set together with the B3LYP functional.

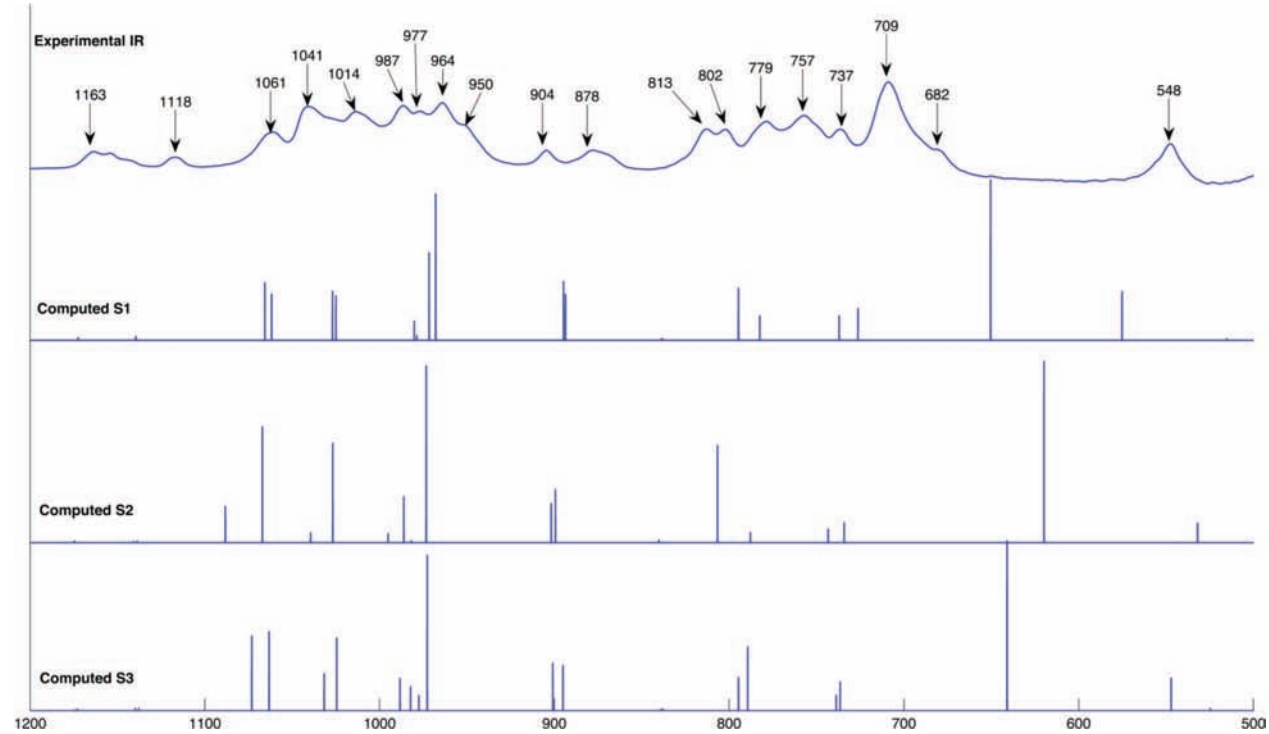

Figure 6. Calculated and experimental vibrational spectra of the S1−S3 conformations, in the 1200−500 cm^{-1} region. 6−311++G(2d, 2p) was used as basis set together with the B3LYP functional.

cal shift, and another is that there is a fast exchange between the different conformations due to the small energy barriers between them. Such an exchange process would lead to signal averaging of the NMR spectrum if it is fast on the NMR time scale.[20] In that case, instead of three signals representing each of the conformations, only one signal is seen, which for symmetrical exchange is positioned at the mean chemical shift of the three signals. The calculated mean values of the chemical shift parameters of S1−S3 give a better overall fit than either of S1, S2, or S3, which could be an indication that there is a symmetrical fast exchange between the three conformations. However, to clarify the situation, relaxation experiments have to be performed, and possibly also more advanced calculations with several molecules involved to investigate whether the hydrocarbon chain movements, and thereby the conformational changes are hindered by neigh-

TABLE 3: Calculated and Experimental ^{31}P Chemical Shift Tensor Parameters of the KDBDTP Salt[b]

structure	δ_{aniso} (ppm)	η	Ω (ppm)	κ	δ_{11} (ppm)	δ_{22} (ppm)	δ_{33} (ppm)	δ_{iso} (ppm)
S1	−120.1	0.09	185.7	0.88	−80.8	−91.7	−266.4	−146.3
S2	−98.9	0.47	171.4	0.46	−75.7	−121.8	−247.1	−148.2
S3	−112.9	0.35	189.2	0.58	−71.3	−111.1	−260.6	−147.7
average	−110.6	0.30	182.1	0.64	−75.9	−108.2	−258.0	−147.4
experimental	−106[a]	0.2[a]	168	0.8	Not directly comparable			
experimental error	±4[a]	±0.2[a]	±9	±0.3				

[a] Larsson et al.[11] [b] 6-311G++(2d, 2p) was used as basis set together with the B3LYP functional.

boring molecules. The results of such investigations will be published elsewhere.

From previous experimental ^{31}P NMR studies on different Metal DTP, a trend was revealed, showing that the principal value δ_{22} of the ^{31}P chemical shift tensor becomes more deshielded when the S−P−S angle increases.[10,11] This relationship was also confirmed by ab initio studies on an [OMeDTP]$^-$ fragment,[11] and the results here showed the same relationship; S1, which has the largest S−P−S angle (Table 1), has the most deshielded value of δ_{22}, whereas S2, which has the smallest S−P−S angle (Table 1), has the most shielded value of δ_{22}. The calculations on the [OMeDTP]$^-$ fragment[11] also implied that the principal value δ_{33} became more shielded when the S−P−S angle increased. The present study showed the same trend, that is a larger S−P−S angle implied more shielding of δ_{33}. This trend was not distinct enough to be confirmed from the ^{31}P CP/MAS NMR experiments on different nickel DTP and zinc DTP complexes[11] but was clear in the study of different lead(II) DTP complexes.[10]

It is interesting to notice, that the mean value of the S−P−S angles of S1−S3 is 118.0°, which is the same as the value for the S−P−S angle of S3 (Table 1). Accordingly, the values of the chemical shift tensor parameters for S3 are similar to the mean values.

5. Conclusions

DFT calculations and IR and NMR experiments have been used to investigate the properties of both the dibutyldithiophosphate anion and its potassium salt. Three different geometrical conformations were considered and geometrical data such as bond lengths and bond angles are presented. Computed vibrational frequencies usually show higher values as compared with recorded spectra. The sum of vibrational frequencies from all conformations S1−S3 is closer to a real infrared spectrum as compared with the spectrum of each conformation separately, indicating that all conformations take part in the formation of the recorded spectrum. The fact that so many conformations with similar energy levels exist can explain the complexity of experimental vibrational spectra because the spectra becomes the sum of the individual spectra of each conformation contributing to it. A shift of up to 25 cm^{-1} in the 900−600 cm^{-1} region was caused by the presence of the metal ion. Furthermore, almost all modes in the region of 1050−750 cm^{-1} are combinations of both stretching of the P−O/P−S bonds and wagging, stretching, or twisting, and rocking modes of the entities within the hydrocarbon chain. ^{31}P CP/MAS NMR chemical shift tensor calculations on S1, S2, and S3 correlate well with experimental data on KDBDTP, especially if the mean value of the sum of the three conformations are considered, suggesting that, a fast, on the NMR time scale, chemical exchange between the conformations takes place. The principal value δ_{22} of the ^{31}P chemical shift tensor becomes more deshielded when the S−P−S angle increases, and δ_{33} becomes more shielded when the S−P−S angle increases. This work clearly shows the high potential of combining DFT modeling and experimental investigations in the interpretation of spectroscopic results. The investigated conformations are a good test of new methods, basis sets or pseudopotentials, because the different conformations are very close in total energy.

Acknowledgment. The authors acknowledge CHEMINOVA A/S for providing the KDBDTP. The DFT calculations were performed at High Performance Computing Center North (HPC2N). The study was financed by Agricola Research Center (ARC), and by its successor ARC-MMS (Multicomponent Mineral Systems), through the Strategic Mining Research Program, cofunded by the Swedish mining industry and the Swedish Governmental Agency for Innovation Systems (VINNOVA).

References and Notes

(1) Antonius, G. F.; Ray, Z. M.; Rivers, L. *J. Environ. Sci. Health, Part B* **2007**, *42*, 9.
(2) Wang, X. B.; Liu, W. M.; Yan, F. Y.; Zhang, Z. J.; Xu, B. S. *Chem. Lett.* **2004**, *33*, 196.
(3) Zhang, Z.; Xue, Q.; Zhang, J. *Wear* **1997**, *209*, 8.
(4) Rao, S. R. *Surface Chemistry of Froth Flotation, Volume 2*, 2nd ed.; Plenum Publishers: New York, 2004.
(5) Ying, X.; Fang, Z. *J. Hazard. Mater.* **2006**, *B137*, 1636.
(6) Jiang, S.; Dasgupta, S.; Blanco, M.; Frazier, R.; Yamaguchi, E. S.; Tang, Y.; Goddard, W. A. *J. Phys. Chem.* **1996**, *100*, 15760.
(7) Yamaguchi, E. S.; Onopchenko, A.; Francisco, M. M.; Chan, C. Y. *Tribol. T.* **1999**, *42*, 895.
(8) Haiduc, I.; Sowerby, D. B.; Lu, S.-F. *Polyhedron* **1995**, *14*, 3389.
(9) Rusanova, D.; Pike, K. J.; Persson, I.; Dupree, R.; Lindberg, M.; Hanna, J. V.; Antzutkin, O. N.; Forsling, W. *Polyhedron* **2006**, *25*, 3569.
(10) Larsson, A.-C.; Ivanov, A. V.; Pike, K. J.; Forsling, W.; Antzutkin, O. N. *J. Magn. Reson.* **2005**, *177*, 56.
(11) Larsson, A.-C.; Ivanov, A. V.; Forsling, W.; Antzutkin, O. N.; Abraham, A. E.; de Dios, A. C. *J. Am. Chem. Soc.* **2005**, *127*, 2218.
(12) Billes, F.; Holmgren, A. *Vib. Spectrosc.* **2005**, *40*, 89.
(13) Mosey, N. J.; Woo, T. K. *Tribol. Int.* **2006**, *39*, 979.
(14) Mosey, N. J.; Woo, T. K. *J. Phys. Chem. A* **2004**, *108*, 6001.
(15) Antzutkin, O. N.; Lee, Y. K.; Levitt, M. H. *J. Magn. Reson.* **1998**, *135*, 144.
(16) Mason, J. *Solid State Nucl. Mag.* **1993**, *2*, 285.
(17) Becke, A. D. *J. Chem. Phys.* **1993**, *98*, 5648.
(18) NW Chem online manual. www.emsl.pnl.gov/docs/nwchem/nwchem.html, June 2008.
(19) Hellström, P.; Fredriksson, A.; Öberg, S.; Holmgren, A. *Spectrochim. Acta A* **2006**, *65*, 887.
(20) Hore, P. J. *Nuclear Magnetic Resonance*; Oxford University Press: Oxford, 1995.

JP805058A